Structure and Mechanism of Spermidine Synthases†

Hong Wu,‡ Jinrong Min,‡ Yoshihiko Ikeguchi,§,|| Hong Zeng,‡ Aiping Dong,‡ Peter Loppnau,‡ Anthony E. Pegg,*,§ and Alexander N. Plotnikov*,‡,⊥

Structural Genomics Consortium, University of Toronto, 100 College Street, Toronto, Ontario, M5G 1L5, Canada, and Department of Cellular and Molecular Physiology, Pennsylvania State University College of Medicine, The Milton S. Hershey Medical Center, P.O. Box 850, 500 University Drive, Hershey, Pennsylvania 17033

Received December 4, 2006; Revised Manuscript Received March 30, 2007

ABSTRACT: Aminopropyltransferases transfer aminopropyl groups from decarboxylated *S*-adenosylmethionine to amine acceptors, forming polyamines. Structural and biochemical studies have been carried out with the human spermidine synthase, which is highly specific for putrescine as the amine acceptor, and the *Thermotoga maritima* spermidine synthase, which prefers putrescine but is more tolerant of other substrates. Comparison of the structures of the human spermidine synthase with both substrates and products with the known structure of *T. maritima* spermidine synthase complexed to a multisubstrate analogue inhibitor and analysis of the properties of site-directed mutants provide a general mechanistic hypothesis for the aminopropyl transfer reaction. The studies also provide a structural basis for the specificity of the spermidine synthase subclass of the aminopropyltransferase family.

Polyamines are ubiquitous and essential cellular components (*1*−*4*). Their synthesis is brought about by enzymes termed aminopropyltransferases (*5*−*8*). These enzymes use an amine acceptor and decarboxylated *S*-adenosylmethionine (dcAdoMet[1]) as the aminopropyl donor. Aminopropyltransferases are of critical importance in the growth and viability of eukaryotes since genetic studies show that spermidine is essential (*1*, *2*, *9*, *10*) and transgenic mice that lack spermine have major developmental and neurological abnormalities (*11*−*13*). *Escherichia coli* can survive without spermidine, but the loss of spermidine synthase (SpdSyn[1]) or *S*-adenosylmethionine (AdoMet[1]) decarboxylase reduces the growth rate and renders the cells more sensitive to oxidative damage (*10*, *14*, *15*). Other microorganisms, particularly those able to grow in extremes of temperature or pH, have a wider variety and very high levels of polyamines, which are needed to allow survival under these conditions (*16*, *17*). The possibility that useful drugs may be obtained by the production of specific inhibitors of aminopropyltransferases is supported by the proven value of inhibitors of earlier stages in the polyamine biosynthetic pathway for the treatment of diseases caused by parasitic protozoa as well as for the prevention of cancer and cancer chemotherapy.

Yeast and higher eukaryotes including plants contain two aminopropyltransferases termed spermidine synthase (SpdSyn[1]) and spermine synthase (*7*, *18*, *19*). The former uses putrescine (1, 4-diaminobutane) as the propylamine acceptor; the latter uses spermidine as acceptor and transfers the propylamine group to the N^8-position forming spermine. Although the reactions brought about by these two enzymes are very similar, most known spermidine synthase proteins including human (HsSpdSyn[1]) are highly specific for putrescine and will not use spermidine as a substrate. Conversely, spermine synthase does not use putrescine. A third class of aminopropyltransferases was revealed recently when it was found that the enzyme from *Thermus thermophilus* uses agmatine rather than putrescine as a substrate (*20*). This provides a novel biosynthetic pathway for spermidine without using putrescine as an intermediate in which the N^1-aminopropylagmatine is converted into spermidine by an ureohydrolase.

The first aminopropyltransferase for which a crystal structure was obtained was the spermidine synthase from *Thermotoga maritima* (TmSpdSyn[1]) (*21*). The complex of this protein with the multisubstrate inhibitor *S*-adenosyl-1,8-diamino-3-thiooctane (AdoDATO[1]) (*22*) showed that the active site contained multiple residues that are highly conserved in known aminopropyltransferases. However, this enzyme has not been fully characterized and no other complexes with substrates or products were reported. We

† This work was supported by the Structural Genomics Consortium with funds from Genome Canada through the Ontario Genomics Institute, the Canadian Institutes for Health Research, the Canada Foundation for Innovation, the Ontario Challenge Fund, the Ontario Innovation Trust, the Wellcome Trust, GlaxoSmithKline, the Knut and Alice Wallenberg Foundation, the Vinnova and Swedish Foundation for Strategic Research, and the United States Public Health Service (Toronto) and by United States Public Health Service Grant R01 GM26290 (Hershey).

* Corresponding authors. A.E.P.: tel, (717) 531-8152; fax, (717) 531-5157; e-mail, aep1@psu.edu. A.N.P.: tel, (416) 946-3868; fax, (416) 946-0588; e-mail, alexander.plotnikov@utoronto.ca.

‡ Structural Genomics Consortium, University of Toronto.

§ Department of Cellular and Molecular Physiology, Pennsylvania State University College of Medicine, The Milton S. Hershey Medical Center.

|| Present address: Department of Biochemistry, Faculty of Pharmaceutical Sciences, Josai University, Sakado, Saitama 350-0295, Japan.

⊥ Department of Physiology, University of Toronto, 112 College Street, Toronto, Ontario M5G 1L6, Canada.

[1] Abbreviations: dcAdoMet, decarboxylated *S*-adenosylmethionine; SpdSyn, spermidine synthase; TmSpdSyn, *T. maritima* spermidine synthase; HsSpdSyn, human spermidine synthase; cadaverine, 1,5-diaminopentane; thermine, *sym*-norspermidine; AdoDATO, *S*-adenosyl-1,8-diamino-3-thiooctane; MTA, 5′-methyl, 5′-deoxymethylthioadenosine; AdoMet, *S*-adenosylmethionine.

10.1021/bi602498k CCC: $37.00
Published on Web 06/22/2007

Table 1: Crystallography Data and Refinement Statistics[a]

	SpdSyn + MTA	SpdSyn + dcAdoMet	SpdSyn + MTA + Put	SpdSyn + MTA + spermidine
		Data Collection		
space group	$P2_1$	$P2_1$	$C222_1$	$P2_1$
cell dimensions				
a, *b*, *c* (Å)	57.93, 60.53, 86.64	58.32,60.59,86.67	119.10, 135.24, 83.32	58.13, 60.66, 86.71
α, *β*, *γ* (deg)	90, 108.42, 90	90, 108.96, 90	90, 90, 90	90, 108.68, 90
resolution (Å)	2.1	2.1	2.1	1.9
R_{merge}	10.5(44.5)	11.3(50.5)	12.6(53.4)	8.8(36.6)
$I/\sigma I$	9.7(2.1)	8.5(2.5)	9.1(3.2)	11.9(2.5)
completeness (%)	99.6 (99.8)	99.3 (100.0)	99.9 (99.9)	97.9 (83.0)
redundancy	3.3 (3.2)	5.3 (5.4)	7.1 (7.0)	4.4 (3.1)
		Refinement		
no. of reflections	31665	31939	37668	42238
R_{work}/R_{free}	18.9/23.7	21.1/27.1	16.6/21.5	17.6/22.8
no. of atoms				
protein	4567	4450	4667	4450
water	289	265	459	624
rms deviations				
bond lengths (Å)	0.014	0.011	0.011	0.017
bond angles (deg)	1.43	1.23	1.27	1.56
PDB code	2O05	2O0L	2O06	2O07

[a] Values in parentheses are for the highest resolution shell.

have now obtained crystal structures of HsSpdSyn with substrate and products and have carried out studies with mutants of key residues of this enzyme. The results provide better understanding of the mechanism of aminopropyl transfer and the substrate specificity of aminopropyltransferases.

EXPERIMENTAL PROCEDURES

Materials. Unlabeled dcAdoMet was kindly provided and synthesized by Professor A. Shirahata (Dept. Biochemistry, Faculty of Pharmaceutical Sciences, Josai Univ., Saitama, Japan). [^{35}S]dcAdoMet was synthesized enzymatically (*23*). Wild type TmSpdSyn and mutants were expressed and purified as previously described (*21*). The mutants were made by using QuikChange Site-directed Mutagenesis kit from Stratagene.

Cloning, Expression, and Purification of HsSpdSyn. A DNA fragment encoding full-length HsSpdSyn was amplified by PCR from the Mammalian Gene Collection clone BC000309 and subcloned into a modified vector (pET28a-LIC) (http://www.sgc.utoronto.ca/SGC-WebPages/toronto-vectors.php), downstream of the poly-histidine coding region. The HsSpdSyn was expressed in *E. coli* BL21 (DE3) codon plus RIL strain (Stratagene). *E. coli* cells carrying the HsSpdSyn expression plasmid were grown at 37 °C to OD_{600} of 1.5 in Terrific Broth (TB) in the presence of 50 μg/mL of kanamycin. Cells were then induced by the addition of 1 mM isopropyl-1-thio-D-galactopyranoside and incubated overnight at 15 °C. Harvested cells were resuspended in lysis buffer (30 mM sodium/potassium phosphate, pH 7.4, 0.25 M NaCl, 5 mM imidazole, 2 mM β-mercaptoethanol, 5% glycerol). The cells were lysed by passing through a microfluidizer (Microfluidics Corp.) at 20,000 psi. After clarification of the crude extract by high-speed centrifugation, the lysate was loaded onto a 5 mL HiTrap chelating column (Amersham Biosciences), charged with Ni^{2+}. The column was washed with 10 column volumes of 20 mM Tris-HCl buffer, pH 8.0, containing 250 mM NaCl, 50 mM imidazole, and 5% glycerol, and the protein was eluted with elution buffer (20 mM Tris-HCl, pH 8.0, 250 mM NaCl, 250 mM imidazole, 5% glycerol). The protein was loaded on a Superdex200 column (26 × 60) (Amersham Biosciences), equilibrated with 20 mM Tris-HCl buffer, pH 8.0, and 150 mM NaCl, at flow rate 4 mL/min. Thrombin (Sigma) was added to combined fractions containing HsSpdSyn to remove His-tag. The protein was further purified to homogeneity by ion-exchange chromatography on a Source 30Q column (Amersham Biosciences), equilibrated with buffer containing 20 mM Tris-HCl, pH 8.0, and eluted with linear gradient of NaCl up to 500 mM concentration.

Crystallization. Purified HsSpdSyn protein was crystallized in the presence of dcAdoMet, MTA, MTA and putrescine, MTA and spermidine, using the hanging drop vapor diffusion method at 20 °C by mixing equal volume of the protein solution (10 mg/mL) with the reservoir solution. HsSpdSyn−MTA complex (protein:MTA molar ratio at 1:5) was crystallized in 20% PEG3350, 0.2 M $Mg(oAC)_2$; HsSpdSyn−dcAdoMet complex (protein:dcAdoMet molar ratio at 1:10) in 25% PEG3350, 0.2 M $MgCl_2$, 0.1 M Tris-HCl, pH 8.5. HsSpdSyn−MTA−putrescine ternary complex (protein:MTA molar ratio at 1:5, protein:putrescine molar ratio at 1:10) was crystallized in 20% PEG3350, 0.2 M ammonium formate; HsSpdSyn−MTA−spermidine ternary complex (protein:MTA and spermidine molar ratio at 1:5) in 25% PEG3350, 0.1 M $(NH_4)_2SO_4$, 0.1 M HEPES-NaOH, pH 7.5.

Data Collection and Structure Determination. X-ray diffraction data were collected at 100 K using Rigaku FRE High Brilliance X-ray generator with R-AXIS IV detector. Data were processed using the HKL software package (*24*). The structures of HsSpdSyn complexes were solved by molecular replacement with the program MOLREP (*25*) using TmSpdSyn as a template (PDB code 1JQ3) (*21*). ARP/wARP was used for automatic model building (*26*). Graphics program COOT (*27*) was used for model building and visualization. Crystal diffraction data and refinement statistics for the structures are displayed in Table 1.

Assay of Aminopropyltransferase Activity. Activity was measured by following the production of [^{35}S]MTA from [^{35}S]dcAdoMet in 100 mM sodium phosphate buffer (pH 7.5), in the presence of the amine acceptor indicated (*23*).

The reaction was stopped by acidification and [^{35}S]MTA separated from [^{35}S]dcAdoMet using phosphocellulose columns (*28*). All assays were conducted with an amount of protein and for a period of time in which product formation was linear with time. Reactions were run with an amount of enzyme that gave a linear rate of MTA production over the assay time period. Assays were conducted for 30 min at 37−50 °C and for 2 min at higher temperatures. The stability of dcAdoMet is reduced at higher temperatures, but even at 80 °C the breakdown of the nucleoside was negligible in 2 min. All assays were carried out in triplicate, and results agreed within ±5%.

RESULTS

Comparison of TmSpdSyn and HsSpdSyn. The structure of HsSpdSyn consists of three domains (Figure 1A): an N-terminal β-strand domain including 6 β-strands, a central catalytic core domain, which has a canonical methyltransferase fold, and a C-terminal α-helix domain including three α-helixes. The first two β-strands of the N-terminal domain form a β-hairpin, followed by a four-strand β-sheet. The structure of HsSpdSyn complexed with the substrate dcAdoMet or the product MTA shows that it is a dimer and that each monomer contains an independent substrate-binding site (Figure 1A). The overall structure of HsSpdSyn from both the binary and ternary structures is almost identical except the loops, which envelop the cofactor and substrate binding sites. The HsSpdSyn dimerizes mainly through the interactions involving the N-terminal domain and the C-terminal domain (Figure 1B). After dimerization, ~1640 Å^2 out of ~13070 Å^2 total surface area for each subunit is buried. The first two β-strands from each subunit of the HsSpdSyn dimer form a distorted 4-strand β-sheet.

TmSpdSyn exists as a tetramer (*21*). However, the molecular structure and orientation of the two subunits in the dimeric HsSpdSyn is very similar to that of TmSpdSyn dimer (Figure 1A). The structure of the HsSpdSyn dimer can be perfectly superimposed with that of either dimer of the TmSpdSyn with an overall root-mean-squared deviation (rmsd) of 1.22 Å. The only major difference in the two structures is the N-terminal domain. Compared to HsSpdSyn, TmSpdSyn has one extra α-helix preceding the N-terminal loop and strand β1. This part is involved in maintaining the TmSpdSyn tetramer structure, while in HsSpdSyn this loop folds back against the core domain of HsSpdSyn (Figure 1A). As described below, the bound substrate/product in HsSpdSyn can also be well superimposed with the equivalent parts of the multisubstrate inhibitor AdoDATO in TmSpdSyn (Figure 1B).

Substrate and Product Binding Sites. The active site of HsSpdSyn is clearly identified by the binding of MTA, dcAdoMet, putrescine, and spermidine (Figures 2, 3). It is formed between the N-terminal domain and the central core domain and is lined with conserved residues in the spermidine synthase family (see Figure S1 in Supporting Information). The active site consists of the dcAdoMet-binding pocket and the amine substrate-binding pocket.

The structure of HsSpdSyn with dcAdoMet (Figure 3A) shows that the nucleoside is bound in the (*S*) form in a negatively charged binding pocket formed by D104, D173, and Q80, which interact with the aminopropyl NH_2 of dcAdoMet, E124 and Q49, which interact with the ribose hydroxyls, and D155, which interacts with 6-NH_2 group of the adenosine moiety. This binding pocket is smaller than the analogous cavity in methyltransferases and contains the charged D104 residue; therefore, it cannot accommodate the AdoMet and use it as a cofactor. The dcAdoMet molecule can be superimposed very well with the MTA molecule in the HsSpdSyn−MTA complex (Figure 3A, B) although MTA lacks the interactions with D104, D173, and Q80.

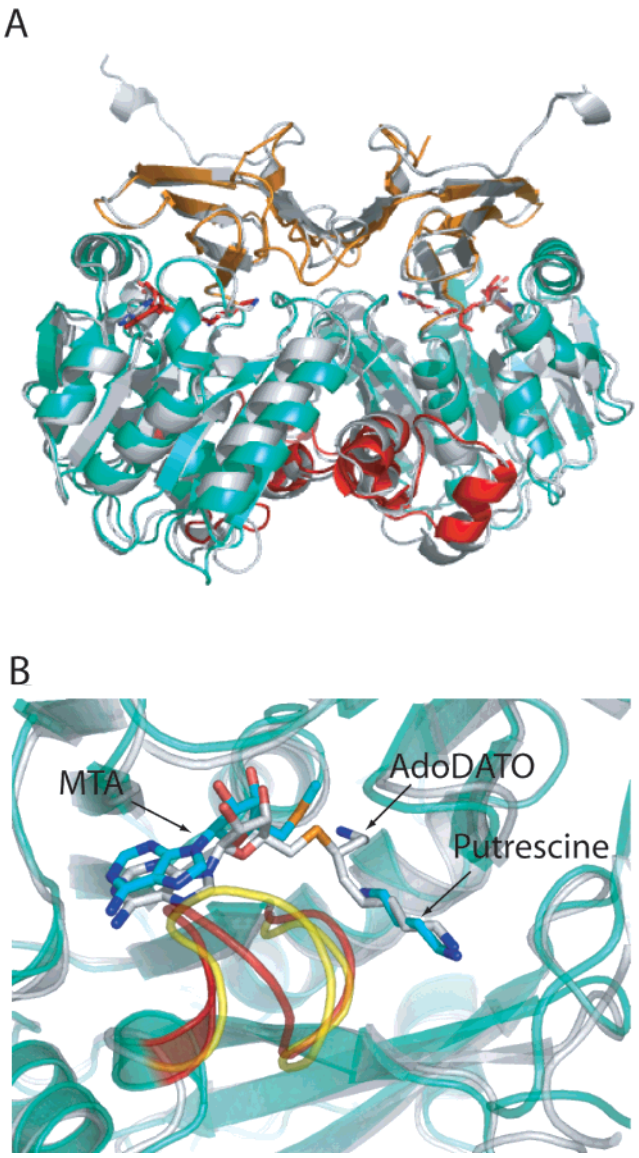

FIGURE 1: Comparison of HsSpdSyn and TmSpdSyn structures. A, Superimposition of HsSpdSyn and TmSpdSyn dimers. All monomers are shown in cartoon diagram representation. The three domains in HsSpdSyn are colored as following: the N-terminal domain is shown in orange, the core domain is shown in greencyan, and the C-terminal domain is shown in red. TmSpdSyn is colored in gray. MTA, putrescine, and AdoDATO are shown in stick representation. Carbon atoms in MTA and putrescine are shown in gray, while AdoDATO is shown in red. B, Superimposition of gate-keeping loops in HsSpdSyn and TmSpdSyn. The HsSpdSyn and TmSpdSyn are shown in cartoon representation, with HsSpdSyn colored in greencyan and TmSpdSyn in gray. The gate-keeping loops are colored in red (for HsSpdSyn) and yellow (for TmSpdSyn). MTA, putrescine, and AdoDATO are shown in stick representation, with carbon atoms in MTA and putrescine colored in cyan and AdoDATO in gray.

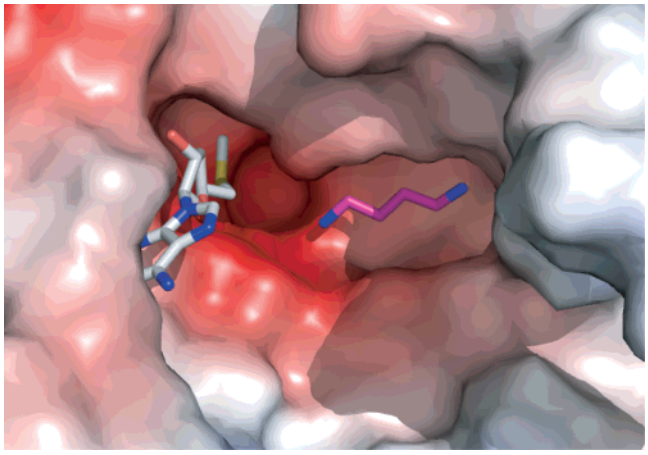

FIGURE 2: Surface of the substrate binding pocket of HsSpdSyn with MTA and putrescine shown in stick representation. Negatively charged surface is colored in red.

Comparison of the active site region in the HsSpdSyn−dcAdoMet structure and the previously published TmSpdSyn−AdoDATO structure (Figure 3A) confirms that (a) the nucleoside moiety of AdoDATO, which was designed as a multisubstrate analogue inhibitor (*29*), does occupy the same position as that of dcAdoMet and that (b) there is a strong conservation of the key residues that make side-chain interactions with the nucleoside. The interactions of E124(Hs), Q49(Hs), and D155(Hs) with the dcAdoMet adenosine moiety are replaced by those of E121(Tm), Q46(Tm), and N152(Tm), respectively. Similarly, the interactions of D104(Hs) and D173(Hs) with the N^1 of the aminopropyl group of dcAdoMet are mimicked by those of D101(Tm) and D170(Tm) with the N^1 of AdoDATO. The other residue involved in dcAdoMet binding, Q80(Hs), is replaced by H77(Tm) in TmSpdSyn and a number of other spermidine synthases (Figure S1 in Supporting Information).

The crystal structure of HsSpdSyn with a putrescine substrate bound could only be obtained when MTA was also present. The putrescine binding pocket revealed by the structure of the HsSpdSyn−MTA−putrescine complex is a narrow channel, which leads to the dcAdoMet binding pocket with the N^1-amino group of putrescine pointing to the sulfur atom of the MTA molecule (Figures 2 and 3C). The surface of the putrescine-binding pocket is weakly negatively charged except the N^1 binding site. The N^1 atom is located in a highly negatively charged environment, and is hydrogen bonded to D173, S174 (backbone), Y79, and Y241 (Figure 3C). This provides an ideal environment for deprotonation of the reactive amino group of putrescine via the postulated reaction mechanism shown in Figure 4. The reactive nitrogen of putrescine points to the sulfur atom directly. To initiate the reaction, the N^1-amino group in putrescine is deprotonated by the aspartic acid (D173) with the aid of other residues (S174, Y79, Y241) for nucleophilic attack on dcAdoMet (Figure 4A). The N^4-amino group of putrescine is hydrogen bonded to D176 (Figures 3C and 4B). This conserved residue is equivalent to D173(Tm), which anchors the N^8-amino group of AdoDATO in the TmSpdSyn−AdoDATO complex (*29*).

The structure of the spermidine molecule in the HsSpdSyn−MTA−spermidine ternary complex, which represents the unreleased products of the reaction, displays a bent conformation (Figure 3D). The N^1 atom of spermidine occupies the same negatively charged binding pocket formed by D104, D173, and Q80 as the dcAdoMet aminopropyl moiety in the HsSpdSyn−dcAdoMet complex structure. The N^8 atom at the other end of spermidine is fixed by D176. However, when the gate-keeping loop (see below) is disordered, the N^8 atom of spermidine forms hydrogen bonds with the carboxylate oxygen of E23 and the backbone carbonyl oxygen of I69, instead of D176. E23 is a fully conserved residue in aminopropyltransferases (Figure S1). The switching of the interacting residues of N^8 atom of spermidine may represent the transition of the product releasing process.

Gate-Keeping Loop. The structure of the TmSpdSyn revealed a highly flexible "gate-keeping" loop made up of amino acids 171−180 which is disordered in the apo-TmSpdSyn structure, but became ordered upon binding of AdoDATO (*29*). Comparisons of the 4 active sites in the TmSpdSyn-AdoDATO tetramer showed a significant conformational change on binding AdoDATO that almost completely covers the inhibitor. This gate-keeping loop is represented by amino acids 174−182 in HsSpdSyn (Figure 1B). It contains part of a short α-helix (α6) in the loop and forms one side of the putrescine binding pocket. In the HsSpdSyn−MTA structure, this gate-keeping loop was still very flexible but was stabilized upon putrescine/spermidine binding. The average *B* factor for this loop in HsSpdSyn−MTA structure is 41−43 Å^2, while in HsSpdSyn−MTA−Put ternary complex structure it is 28 Å^2 and in HsSpdSyn−MTA−Spd ternary complex structure it is 29 Å^2.

Based on the available structures, we propose that the loops enveloping the active site (or the loops forming the entrance to the active site) are very flexible and exposed to solvent in the apo spermidine synthases. Binding of the nucleoside and amine substrates facilitates the formation of the active site, which becomes almost solvent inaccessible in the binary structures.

Amine Substrate Specificity. The HsSpdSyn was highly specific for putrescine as an amine acceptor. Less than 5% activity was observed using 1,3-diaminopropane, and <1% activity was seen with larger substrates such as spermidine. This strict specificity is similar to that previously reported for other SpdSyns from plants, *E. coli*, rats, and pigs (*6*, *30*−*32*). Kinetic analysis of the HsSpdSyn reaction indicated that the K_m values for putrescine and dcAdoMet were 20 μM and 0.9 μM, respectively, and that the k_{cat} was 1.9 s^{-1} (Table 2). These values are also similar to those in the literature for other mammalian SpdSyns and *E. coli* SpdSyn which have been reported to have K_m values of 1−3 μM for dcAdoMet and 12−40 μM for putrescine and k_{cat} values of 0.5−2 s^{-1} (*6*, *30*−*32*).

As shown in Table 2, the kinetic parameters for TmSpdSyn at 37 °C with putrescine as a substrate were very similar to those of the other known SpdSyns (including HsSpdSyn) with K_m values of 19 μM for putrescine and 0.75 μM for dcAdoMet and a k_{cat} of c. 0.8 s^{-1} (Table 2). As expected, the TmSpdSyn was remarkably stable to thermal denaturation with a $t_{1/2}$ of 13 h at 90 °C whereas HsSpdSyn has a $t_{1/2}$ of <1 min at 90 °C. The k_{cat} value for TmSpdSyn increased greatly as the assay temperature increased (Table 2 and Figure 5).

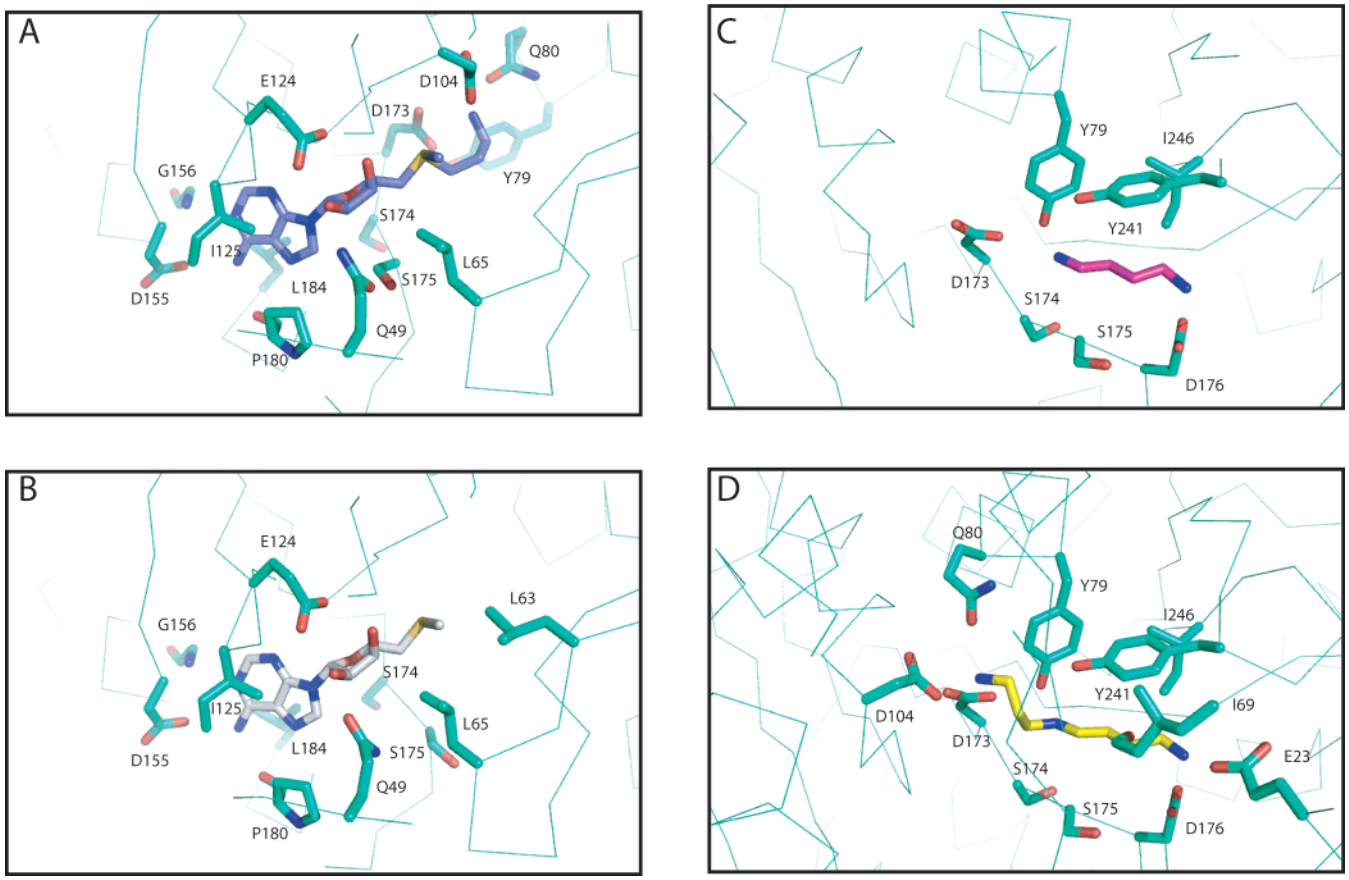

FIGURE 3: Interactions between HsSpdSyn and its substrates and reaction products. All residues that interact with the compounds are shown in stick representation. The residues are labeled individually, and the carbon atoms are colored in greencyan. A, Interactions between HsSpdSyn and dcAdoMet. Carbon atoms in dcAdoMet are colored in purple. B, Interactions between HsSpdSyn and MTA. Carbon atoms in MTA are colored in gray. C, Interactions between HsSpdSyn and putrescine. Carbon atoms in putrescine are colored in magenta. Residue D173, which interacts with both dcAdoMet and putrescine, is shown in both panels A and C. D, Interactions between HsSpdSyn and spermidine. Carbon atoms in spermidine are colored in yellow. The residues interacting with N^8 atom of spermidine in ordered (D176) and disordered (E23 and I69) form are all shown.

The TmSpdSyn was able to use other amines as acceptors of the aminopropyl group in contrast to the results with HsSpdSyn. Substrates included 1,3-diaminopropane, 1,5-diaminopentane (cadaverine), agmatine, *sym*-norspermidine (thermine), and spermidine. This was not an artifact of the assay being conducted at 37 °C, which is far from the optimum temperature, as it was also seen at higher temperatures (Figure 5). The reaction rate for all of these substrates increased at higher temperatures but in all cases was less than with putrescine (Figure 5B). In fact, except for spermidine, the relative rate compared to putrescine went down with increasing temperature for these alternative substrates. At 37 °C, the maximal reaction with spermidine occurred at 18% of the rate with putrescine and the corresponding values for the other amines were thermine (37%), 1,3-diaminopropane (23%), and 1,5-diaminopentane (4%). At 65 °C, the relative rates were spermidine (31%), thermine (15%), 1,3-diaminopropane (11%) and 1,5-diaminopentane (8%). A full analysis was not undertaken for these substrates, but the K_m values were much higher than for putrescine at all temperatures. Thus, TmSpdSyn is definitely a spermidine synthase but is promiscuous compared to other characterized SpdSyn proteins such as *E. coli*, yeast, and mammalian including HsSpdSyn (*6*, *7*).

Comparison of the structures of the HsSpdSyn with bound putrescine or spermidine with that of TmSpdSyn provides a basis for the greater amine substrate specificity. As previously suggested (*7*), steric factors prevent the binding of longer substrates such as thermine and spermidine to the position occupied by putrescine in the likely substrate binding mode (see above). Such binding places the additional aminopropyl group of other longer substrates in a region occupied by W28 in HsSpdSyn, and the W28 side chain closes off the substrate binding pocket. In contrast, the binding cavity in TmSpdSyn is restricted by residue Y23 but not in a way that would totally exclude larger substrates (Figure 6). The greater activity of the TmSpdSyn toward diamines other than putrescine such as 1,3-diaminopropane and cadaverine is likely to be due to the greater flexibility in the gate-keeping loop described above. In TmSpdSyn this loop contains one more residue (T175) and lacks the proline equivalent to P180(Hs), which is also present in other more specific spermidine synthases (Figure S1). In TmSpdSyn, this proline is replaced by a glutamine (Q178).

Effect of Alteration of Key Active Site Residues. Alterations were made by site-directed mutagenesis to the key residues D101, D170, D173, and Y76 in TmSpdSyn, which are equivalent to residues D104, D173, D176, and Y79 in the HsSpdSyn structure. These residues interact with substrates as shown in Figures 3 and 4.

Residue D101(Tm) equivalent to D104(Hs) is a totally conserved residue in all known aminopropyltransferases. The

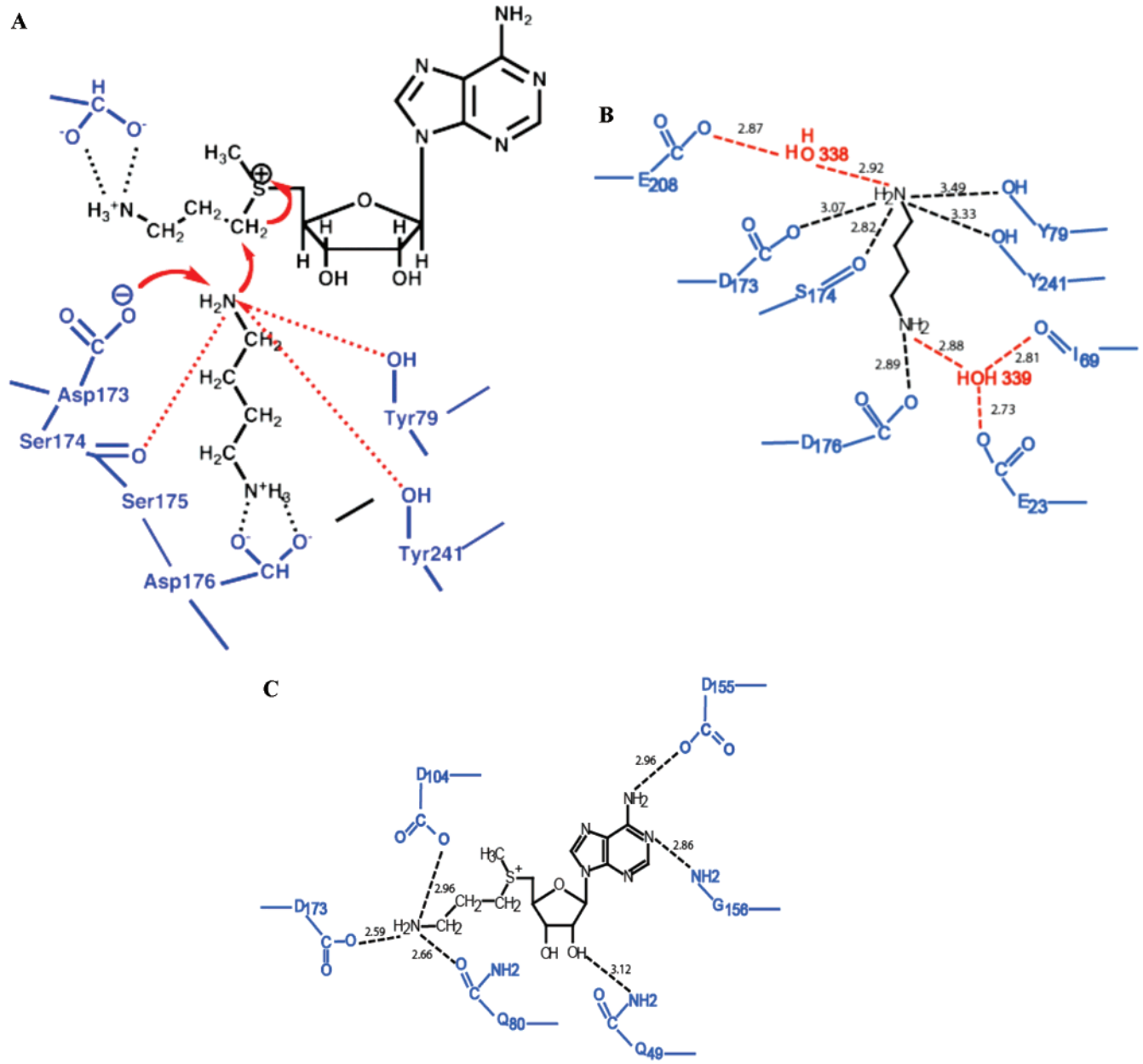

FIGURE 4: General mechanism for aminopropyl transfer. Panel (A) shows the proposed mechanism. The putrescine and dcAdoMet substrates are shown in black. The proposed attack by the putrescine amino group on the methylene carbon of the aminopropyl group is indicated by red arrows. This attack is facilitated by interactions of amino group with the side chain of Y79 and D173 and the carbonyl group of S174 which deprotonate the attacking amino group. Both amino groups of putrescine would be expected to be protonated in solution at neutral pH based on the pK_a values of 10.8 and 9.3 (*44*). Residue D176, which bonds with the other charged amino group of putrescine, and D104, which bonds with the amino group on dcAdoMet, are also shown. Based on pK_a values these amino groups would be expected to be charged and are shown as such with interactions to the carboxyl groups of D176 and D104. Residues in HsSpdSyn are shown in blue and interactions as black or red dotted lines. Panels (B) and (C) show the H bonds indicated by the crystal structure for putrescine (B) and dcAdoMet (C) including those intermediated by water (shown in red).

Table 2: Comparison of HsSpdSyn and TsSpdSyn

protein	K_m putrescine at 37 °C (μM)	K_m dcAdoMet at 37 °C (μM)	k_{cat} at 37 °C (s^{-1})	k_{cat} at 80 °C (s^{-1})
wild type HsSpdSyn	20	0.9	1.9	inactive
wild type TmSpdSyn	19	0.75	0.77	22.7

acidic side chain is located within hydrogen-bonding distance of the terminal amino group of the dcAdoMet substrate in HsSpdSyn (Figures 3A and 4C). This residue is replaced by isoleucine in putrescine-*N*-methyltransferase (*33*). Mutant D101I was much less active than wild type TmSpdSyn, and this alteration produced a large increase in K_m for dcAdoMet (>100-fold) and a >50,000-fold reduction in k_{cat}/K_m (Table 3).

As suggested above and diagramed in Figures 3C and 4B, Y76, D170, and D173 in TmSpdSyn (Y79, D173, and D176 in HsSpdSyn, respectively) are likely to play a critical part in putrescine binding and the transfer reaction. Mutants Y76F, D170A, and D173A were all much less active than wild type TmSpdSyn (Table 3). The K_m values for putrescine were increased by all of these mutations by 12-fold, 240-fold, and 45-fold respectively. This is consistent with a role for these residues in interaction with putrescine as shown in

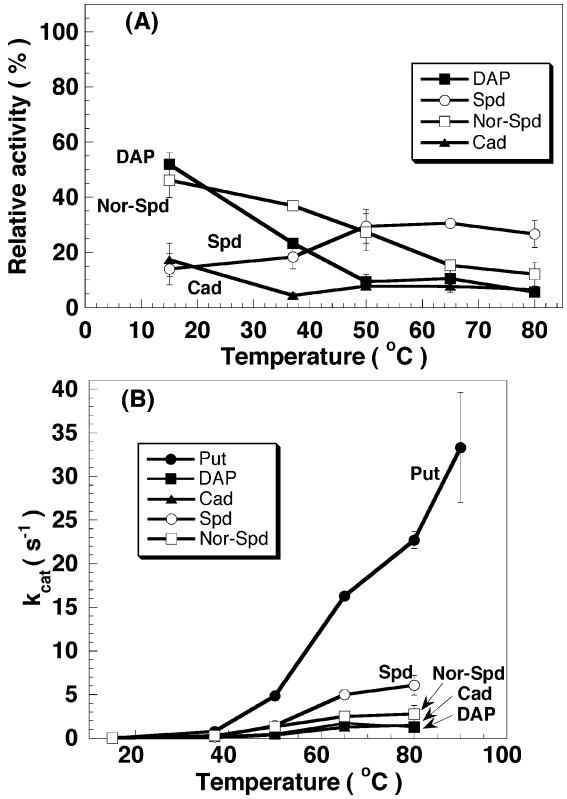

FIGURE 5: Effect of temperature on formation of spermidine and other polyamines by TmSpdSyn. The assays were carried out as described under Methods and Materials at the temperature shown for putrescine (Put) 1,3-diaminopropane (DAP); 1,5-diaminopentane (cadaverine, Cad); thermine (*sym*-norspermidine, Nor-Spd); and spermidine (Spd). The results are shown as the mean ± SD for at least 3 estimations. The SD was less than the size of the symbols in some assays. Measurements at 90 °C were hampered by the instability of dcAdoMet at this temperature. Therefore, the assays with other substrates were carried out over the range from 15 °C to 80 °C. Panel A shows the relative activities of the k_{cat} values for other substrates compared to that for putrescine (set at 100%) at each temperature. Panel B shows the effect of temperature on k_{cat}.

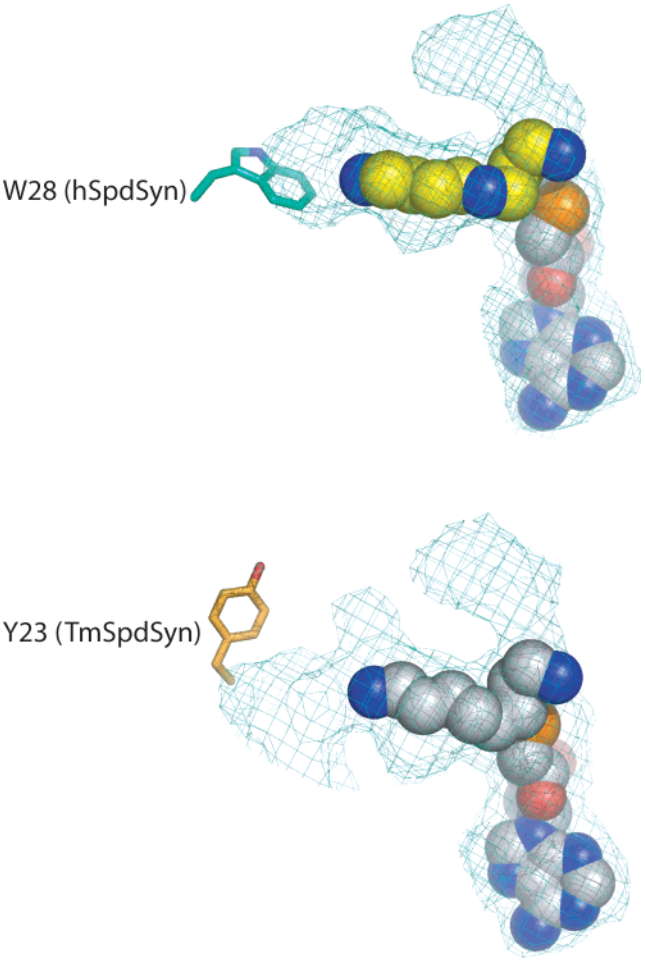

FIGURE 6: Active site of HsSpdSyn highlighting the end of spermidine binding pocket. In HsSpdSyn (upper panel), the cavity is closed off by W28. By contrast, this region in TmSpdSyn (lower panel) is more open due to the position of Y23. Shown in green mesh is the surface of HsSpdSyn or TmSpdSyn within 4 Å of spermidine and MTA or AdoDATO, respectively. Spermidine, MTA, and AdoDATO are shown in sphere representation. Carbon atoms in spermidine and MTA in HsSpdSyn structure are colored in yellow and gray, respectively. Carbon atoms in AdoDATO in TmSpdSyn structure are colored in gray. W28 of HsSpdSyn and Y23 of TmSpdSyn are shown in stick representation with carbon atoms colored in greencyan and orange, respectively.

Figure 4. These mutations had much smaller but significant effects of the K_m for dcAdoMet, which was increased by 6.4-fold, 3.3-fold, and 2-fold, respectively. The k_{cat}/K_m values were all greatly reduced by these mutations with D170A producing the greatest effect (a >10,000-fold reduction). This is consistent with the postulated role for this residue in the deprotonation of the reactive amino group of putrescine shown in Figure 4A. The D173A mutant had a reduction in k_{cat}/K_m of >500-fold, and the Y76F mutant had a reduction of >1000-fold. When the activity was measured at 80 °C rather than 37 °C, the relative order of the differences in k_{cat} was maintained but the magnitude of the reduction was lessened for Y76F and D173A.

Table 3: Effect of Mutations in Active Site Pocket on Reaction of TmSpdSyn

protein	k_{cat}/K_m putrescine at 37 °Ca (s^{-1}/M^{-1})	k_{cat}/K_m dcAdoMet at 37 °C (s^{-1}/mM^{-1})[a]	k_{cat} at 37 °C (s^{-1})	k_{cat} at 80 °C (s^{-1})
wild type TmSpdSyn	40526	1027	0.77	22.7
D101I TmSpdSyn	2.7	<0.02	0.0004	0.012
Y76F TmSpdSyn	21.5	1.04	0.005	8.1
D170A TmSpdSyn	0.03	0.06	0.00015	0.014
D173A TmSpdSyn	3.5	2.00	0.003	1.5

[a] Units are changed for convenience in presentation.

DISCUSSION

SpdSyn is an essential enzyme for growth of all eukaryotes. Deletion of the *SpdS* gene in *Saccharomyces cerevisiae* (*34*), *Dictyostelium discoideum* (*35*), *Leishmania donovani* (*36*), *Aspergillus nidulans* (*37*), and *Cryptococcus neoformans* (*38*) results in strains requiring spermidine for growth. The inactivation of the mouse *AdoMetDC* gene that provides the dcAdoMet substrate for spermidine production is lethal at an early stage of development (*2*). This is not due to prevention of spermine synthase activity since mice with this gene inactivated are viable (*7*). Spermidine synthase is the only other protein known to use dcAdoMet as a substrate. Following the publication of the structure of TmSpdSyn (*21*) several other aminopropyltransferase structures are now available including those of the spermidine synthases from *Caenorhabditis elegans* (PDB: 2B2C) (*39*), *Arabidopsis*

thaliana (PDB: 1XJ5), *Bacillus subtilis* (PDB: 1IY9), *Pyrococcus furiosus* (PDB: 1MJF), *P. falciparum* (PDB: 2HTE), and the *Thermus thermophilus* aminopropylagmatine synthase (PDB: 1UIR) (*20*). However, with the exception of the TmSpdSyn and *P. falciparum* structures complexed with AdoDATO or MTA, none of these structures have complexes with substrates or inhibitors. The data presented here are the first spermidine synthase structures that contain all four substrates and products.

These structures and the previous structures of AdoDATO complexes allow the general mechanism for the aminopropyltransferase reaction to be postulated according to the scheme shown in Figure 4A. Three aspartic acid residues in human spermidine synthase (D104, D173, and D176), which are conserved in all spermidine synthase structures, play key essential roles in the aminopropyltransferase reaction. This is indicated both by the structures shown in Figure 3 and the results of the site-directed mutagenesis shown in Table 3. The carboxylate side chain of D173 plays a major role in the deprotonation of the substrate and is aided in this by the backbone carbonyl of S174 and the hydroxyl groups from Y79 and Y214, which are also fully conserved. The carboxylate side chain of D176 is required for correct binding of putrescine by fixing the distal end of the diamine. The carboxylate of D104 binds both the aminopropyl end of dcAdoMet and the N^1 atom of spermidine. D104 facilitates the initiation of the nucleophilic attack on dcAdoMet by anchoring the aminopropyl group and restricting it in the position for reaction to start. After completion of the transfer of the aminopropyl group from dcAdoMet to putrescine, the aminopropyl group in spermidine still occupies the pocket consisting of D104, D173, and Q80 until the product is released. The roles of some other highly conserved residues such as E124 and Q49, which interact with the substrate ribose, are also explained by the current crystal structures.

The mechanism described above is in accordance with previous studies showing that the reaction is a bimolecular displacement (*40*, *41*). The generality of this mechanism is supported by the site-directed mutagenesis experiments shown in Table 3 with the TmSpdSyn, which, as described above, has a wider amine acceptor substrate specificity. It is therefore likely to apply to all aminopropyltransferases including spermine synthases and aminopropylagmatine synthases. All gene sequences for these proteins contain conserved residues corresponding to the key Asp residues 104(Hs) and 173(Hs) (Figure S1).

The structure of HsSpdSyn−dcAdoMet complex shows that the protein uses the (*S*) isomer of dcAdoMet at the sulfonium center. The (*S,S*) form of AdoMet is the diastereomer that is produced enzymatically *in vivo*, but spontaneous conversion to a mixture with the (*R,S*) isomer occurs naturally. The (*S,S*) form appears to be the biologically active material and is the form that is used by AdoMet decarboxylase (*42*) so the use of (*S*)dcAdoMet by spermidine synthase is consistent with these results. Most enzymes using AdoMet bind the substrate in a configuration that has a torsion angle corresponding to the *anti* configuration at the glycosidic bond, which is also the predominant form in solution (*43*), but AdoMetDC is quite unusual in that the substrate and product are bound in the *syn*-conformation (*42*). However, HsSpdSyn resembles methyltransferases in that the bound nucleoside is clearly in the *anti*-configuration.

Our results also provide a convincing explanation for the difference in amine substrate specificity between the HsSpdSyn, which is highly specific for putrescine, and TmSpdSyn, which is less specific and will use longer substrates including spermidine and thermine (Figure 5). The base of the amine binding pocket in HsSpdSyn is fully blocked by the side chain of W28 preventing the binding of spermidine. In TmSpdSyn, this area is more open and can allow binding of longer substrates although it is somewhat restricted by Y23 explaining the preference for diamines. The increased size of the flexible substrate binding loop in TmSpdSyn which contains one more residue and one less proline than the HsSpdSyn provides a plausible explanation for the greater ability of the former to use diamines other than putrescine as substrate.

The flexible gate-keeping loop is clearly a critical feature of spermidine synthases. It is likely that movement of this loop upon binding substrates places the putrescine in the correct position for reaction to take place. This loop must open again in order for product release. The mechanism underlying this opening is not fully addressed by our experiments, but the ability of the N^8-end of the reaction product spermidine to interact with fully conserved residue E23 and D176 in different conformation of this loop may contribute to this opening, thereafter to the release of the reaction products.

ACKNOWLEDGMENT

We thank Dr. Alexei Savchenko for providing the mutants of TmSpdSyn used in this study and Drs. Aled Edwards, Cheryl Arrowsmith, and Natalia A. Loktionova for critical reading of the manuscript.

SUPPORTING INFORMATION AVAILABLE

Multiple sequence alignment of spermidine synthases is shown in Figure S1. This material is available free of charge via the Internet at http://pubs.acs.org.

REFERENCES

1. Pendeville, H., Carpino, N., Marine, J. C., Takahashi, Y., Muller, M., Martial, J. A., and Cleveland, J. L. (2001) The ornithine decarboxylase gene is essential for cell survival during early murine development, *Mol. Cell Biol. 21*, 6459−6558.
2. Nishimura, K., Nakatsu, F., Kashiwagi, K., Ohno, H., Saito, H., Saito, T., and Igarashi, K. (2002) Essential role of *S*-adenosylmethionine decarboxylase in mouse embryonic development, *Genes Cells 7*, 41−47.
3. Gerner, E. W., and Meyskens, F. L., Jr. (2004) Polyamines and cancer: old molecules, new understanding, *Nat. Rev. Cancer 4*, 781−792.
4. Jänne, J., Alhonen, L., Pietilä, M., and Keinänen, T. (2004) Genetic approaches to the cellular functions of polyamines in mammals, *Eur. J. Biochem. 271*, 877−894.
5. Pegg, A. E. (1986) Recent advances in the biochemistry of polyamines in eukaryotes, *Biochem. J. 234*, 249−262.
6. Pegg, A. E., Poulin, R., and Coward, J. K. (1995) Use of aminopropyltransferase inhibitors and of non-metabolizable analogues to study polyamine regulation and function, *Int. J. Biochem. 27*, 425−442.
7. Ikeguchi, Y., Bewley, M., and Pegg, A. E. (2006) Aminopropyltransferases: function, structure and genetics, *J. Biochem. 139*, 1−9.
8. Wallace, H. M., Fraser, A. V., and Hughes, A. (2003) A perspective of polyamine metabolism, *Biochem. J. 376*, 1−14.
9. Park, M. H., Lee, Y. B., and Joe, Y. A. (1997) Hypusine is essential for eukaryotic cell proliferation, *Biol. Signals 6*, 115−123.

10. Chattopadhyay, M. K., Tabor, C. W., and Tabor, H. (2003) Spermidine but not spermine is essential for hypusine biosynthesis and growth in Saccharomyces cerevisiae: spermine is converted to spermidine in vivo by the FMS1-amine oxidase, *Proc. Natl. Acad. Sci. U.S.A. 100*, 13869−13874.
11. Lorenz, B., Francis, F., Gempel, K., Böddrich, A., Josten, M., Schmahl, W., and Schmidt, J. (1998) Spermine deficiency in Gy mice caused by deletion of the spermine synthase gene, *Hum. Mol. Genet. 7*, 541−547.
12. Wang, X., Ikeguchi, Y., McCloskey, D. E., Nelson, P., and Pegg, A. E. (2004) Spermine synthesis is required for normal viability, growth and fertility in the mouse, *J. Biol. Chem. 49*, 51370−51375.
13. Mackintosh, C. A., and Pegg, A. E. (2000) Effect of spermine synthase deficiency on polyamine biosynthesis and content in mice and embryonic fibroblasts and the sensitivity of fibroblasts to 1,3-bis(2-chloroethyl)-N-nitrosourea, *Biochem. J. 351*, 439−447.
14. Xie, Q.-W., Tabor, C. W., and Tabor, H. (1993) Deletion mutation in the speED operon: spermidine is not essential for the growth of Escherichia coli, *Gene 126*, 115−117.
15. Chattopadhyay, M. K., Tabor, C. W., and Tabor, H. (2003) Polyamines protect Escherichia coli cells from the toxic effect of oxygen, *Proc. Natl. Acad. Sci. U.S.A. 100*, 2261−2265.
16. Hamana, K., Niitsu, M., Samejima, K., and Itoh, T. (2001) Polyamines of the thermophilic eubacteria belonging to the genera *Thermosipho*, *Thermabacter* and *Caldicellulosiruptor*, *Microbios 104*, 177−185.
17. Terui, Y., Ohnuma, M., Hiraga, K., Kawashima, E., and Oshima, T. (2005) Stabilization of nucleic acids by unusual polyamines produced by an extreme thermophile, *Biochem. J. 388*, 427−433.
18. Hamasaki-Katagiri, N., Katagiri, Y., Tabor, C. W., and Tabor, H. (1998) Spermine is not essential for growth of *Saccharomyces cerevisiae*: identification of the *SPE4* gene (spermine synthase) and characterization of a *spe4* deletion mutant, *Gene 210*, 195−210.
19. Hanzawa, Y., Imai, A., Michael, A. J., Komeda, Y., and Takahashi, T. (2002) Characterization of the spermidine synthase-related gene family in *Arabidopsis thaliana*, *FEBS Lett. 527*, 176−180.
20. Ohnuma, M., Terui, Y., Tamakoshi, M., Mitome, H., Niitsu, M., Samejima, K., Kawashima, E., and Oshima, T. (2005) N^1-Aminopropylagmatine: A new polyamine produced as a key intermediate in polyamine biosynthesis of an extreme thermophile, *Thermus thermophilus*, *J. Biol. Chem. 280*, 30073−30082.
21. Korolev, S., Ikeguchi, Y., Skarina, T., Beasley, S., Arrowsmith, C., Edwards, A., Joachimiak, A., Pegg, A. E., and Savchenko, A. (2002) The crystal structure of spermidine synthase with a multisubstrate adduct inhibitor, *Nat. Struct. Biol. 9*, 27−31.
22. Tang, K. C., Pegg, A. E., and Coward, J. K. (1980) Specific and potent inhibition of spermidine synthase by the transition-state analog, S-adenosyl-3-thio-1,8-diaminooctane, *Biochem. Biophys. Res. Commun. 96*, 1371−1377.
23. Wiest, L., and Pegg, A. E. (1998) Assay of spermidine and spermine synthase, in *Methods in Molecular Biology. 79. Polyamine Protocols* (Morgan, D. M. L., Ed.) pp 51−58, Humana Press, Totowa, NJ.
24. Otwinowski, Z. M. W. (1997) Processing of X-ray diffraction data collected in oscillation mode, *Methods Enzymol 276*, 307−326.
25. Vagin, A. T. A. (1997) MOLREP: an Automated Program for Molecular Replacement, *J. Appl. Crystallogr. 30*, 1022−1025.
26. Perrakis, A., Harkiolaki, M., Wilson, K. S., and Lamzin, V. S. (2001) ARP/wARP and molecular replacement, *Acta Crystallogr., Sect. D: Biol. Crystallogr. 57*, 1445−1450.
27. Emsley, P., and Cowtan, K. (2004) Coot: Model-building tools for molecular graphics, *Acta Crystallogr. D60*, 2126−2132.
28. Pegg, A. E. (1983) Assay of aminopropyltransferases, *Methods Enzymol. 94*, 260−265.
29. Tang, K. C., Mariuzza, R., and Coward, J. K. (1981) Synthesis and evaluation of some stable multisubstrate adducts as specific inhibitors of spermidine synthase, *J. Med. Chem. 24*, 1277−1284.
30. Samejima, K., and Yamanoha, B. (1982) Purification of spermidine synthase from rat ventral prostate by affinity chromatography on immoblized S-adenosyl(5′)-3-thiopropylamine, *Arch. Biochem. Biophys. 216*, 213−222.
31. Raina, A., Hyvonen, T., Eloranta, T., Voutilainen, M., Samejima, K., and Yamanoha, B. (1984) Polyamine synthesis in mammalian tissues. Isolation and characterization of spermidine synthase from bovine brain, *Biochem. J. 219*, 991−1000.
32. Tabor, C. W., and Tabor, H. (1983) Putrescine aminopropyltransferase (Escherichia coli), *Methods Enzymol. 94*, 265−270.
33. Riechers, D. E., and Timko, M. P. (1999) Structure and expression of the gene family encoding putrescine N-methyltransferase in Nicotiana tabacum: new clues to the evolutionary origin of cultivated tobacco, *Plant Mol. Biol. 41*, 387−401.
34. Hamasaki-Katagiri, N., Tabor, C. W., and Tabor, H. (1997) Spermidine biosynthesis in *Saccharomyces cerevisiae*: polyamine requirement of a null mutant of the *SPE3* gene (spermidine synthase), *Gene 187*, 35−43.
35. Guo, K., Chang, W.-T., and Newell, P. C. (1999) Isolation of spermidine synthase gene (*spsA*) of *Dictyostelium discoideum*, *Biochim. Biophys. Acta 1449*, 211−216.
36. Roberts, S. C., Jiang, Y., Jardim, A., Cater, N. S., Heby, O., and Ullman, B. (2001) Genetic analysis of spermidine synthase from *Leishmania donovani*, *Mol. Biochem. Parasitol. 115*, 217−226.
37. Jin, Y., Bok, J. W., Guzman-de-Pena, D., and Keller, N. P. (2002) Requirement of spermidine for developmental transitions in Aspergillus nidulans, *Mol. Microbiol. 46*, 801−812.
38. Kingsbury, J. M., Yang, Z., Ganous, T. M., Cox, G. M., and McCusker, J. H. (2004) Novel chimeric spermidine synthase-saccharopine dehydrogenase gene (SPE3-LYS9) in the human pathogen Cryptococcus neoformans, *Eukaryotic Cell 3*, 752−763.
39. Dufe, V. T., Luersen, K., Eschbach, M. L., Haider, N., Karlberg, T., Walter, R. D., and Al-Karadaghi, S. (2005) Cloning, expression, characterisation and three-dimensional structure determination of *Caenorhabditis elegans* spermidine synthase, *FEBS Lett. 579*, 6037−6043.
40. Golding, B. T., and Nassereddin, I. K. (1985) The biosynthesis of spermidine. Part 3: The stereochemistry of the formation of the N-CH_2 group in the biosynthesis of spermidine, *J. Chem. Soc., Perkin Trans. 1*, 2017−2024.
41. Orr, G. J., Danz, D. W., Pontoni, G., Prabhakaran, P. C., Gould, S. J., and Coward, J. K. (1988) Synthesis of chirally deuteriated (S-adenosyl-S-methylsufonio)propylamines and spermidines. Elucidation of the stereochemical course of putrescine aminopropyltransferase (spermidine synthase), *J. Am. Chem. Soc. 110*, 5791−5799.
42. Tolbert, D. W., Ekstrom, J. L., Mathews, I. I., Secrist, J. A. I., Kapoor, P., Pegg, A. E., and Ealick, S. E. (2001) The structural basis for substrate specificity and inhibition of human S-adenosylmethionine decarboxylase, *Biochemistry 40*, 9484−9494.
43. Markham, G. D., Norrby, P.-O., and Bock, C. W. (2002) S-Adenosylmethionine conformations in solution and in protein complexes:conformational influences of the sulfonium group, *Biochemistry 41*, 7636−7646.
44. Takeda, Y., Samejima, K., Nagano, K., Watanabe, M., Sugeta, H., and Kyogoku, Y. (1983) Determination of protonation sites in thermospermine and in some other polyamines by 15N and 13C nuclear magnetic resonance spectroscopy, *Eur. J. Biochem. 130*, 383−389.

BI602498K